Fermi National Accelerator Laboratory

FERMILAB-Pub-89/186-A
September 1989

COSMIC STRING INDUCED HOT DARK MATTER PERTURBATIONS

Anthony van Dalen

Department of Physics
University of Chicago, Chicago, IL 60637
and
NASA/Fermilab Astrophysics Center, P.O. Box 500 Batavia, IL 60510

Abstract

A detailed analysis is presented of the linear evolution of spherical perturbations in a Universe dominated today by light interactionless particles. This formalism is used to study the evolution of perturbations around a sphere of uniform density and fixed radius, approximating a loop of cosmic string, plus a compensating perturbation in gravitational radiation. On small scales the results agree with the nonrelativistic calculation of previous authors. On scales greater than a few megaparces there is a deviation aproaching a factor of 2 to 3 in the perturbation mass. The difference is mainly due to the inclusion of the photon/baryon fluid before decoupling. A scenario with cosmic strings, hot dark matter and a Hubble constant greater than 75 km/s/Mpc can generally produce structure on the observed mass scales and at the appropriate time: $1+z \approx 4$ for galaxies and $1+z \approx 1.5$ for Abell clusters. For a Hubble constant of 50 km/s/Mpc, galaxies can still be seeded but they are considerably smaller for a given seed mass. The fact that recent simmulations indicate a much larger string density than previously determined makes this a favorable effect. This success is to be contrasted with the hot dark matter plus Gaussian fluctuation model where clusters can be easily accounted for but structure on the scale of galaxies is smoothed out by free-streaming. The work presented here does not include the effect of seed loop peculiar velocities. However, as with a Newtonian potential, one can integrate the spherically symmetric solution to determine the effect of a perturbation of arbitrary initial geometry.

Accepted for publication in the Ap. J.

1. Introduction

In this paper the evolution of initially relativistic matter, radiation and baryons around cosmic string seed perturbations is investigated. In setting up a solution for this problem the formalism for evolving spherically symmetric perturbations from the early universe to the present is developed.

The 'standard' hot dark matter model has a number of appealing features: The dominant mass component of the Universe has three candidates that are known to exist (the neutrinos), and power on large scales to produce both streaming velocities (Dressler *et al.* 1987) and positive correlation functions (Bahcall and Soneira 1983). Unfortunately, one pays for the large scale power by washing out any primordial structure on smaller scales, making galaxy formation possible only at a very recent epoch (Peebles 1982, Frenk, White, and Davis 1983, and Bond and Szalay 1983). One could avoid this problem if the primordial structure was in some kind of cold material, such as cosmic string. In this model the neutrinos are free to move around while they are hot, but as the Universe cools they will eventually accrete onto the string seeds to form galaxies.

Cosmic strings occur naturally in many particle physics models (Kibble 1976). To form strings requires a symmetry breaking phase transition involving a complex scalar Higgs field. To produce objects massive enough to seed structure in the Universe this transition must be near the grand unification scale. After the transition one is left with a network of essentially one dimensional concentrations of stress energy that fill the Universe like a collection of random walk trajectories. One might be concerned that these strings would come to dominate the energy density of the Universe, however, simulations (Albrecht and Turok 1985; Bennett and Bouchet 1988) indicate that once decoupled from the background long strings will be continuously breaking off loops which subsequently slowly decay into gravitational radiation. The whole network of strings scales like radiation and thus do not significatly affect the large scale evolution of the Universe. However, on smaller scales the chopped-off loops pose reasonable candidates for the seeds of galaxies and clusters (Zel'dovich 1980; Vilenkin 1981).

Theories with strings and cold dark matter (CDM) have been considered by Sato (1986), Stebbins (1986), and Turok and Brandenberger (1986). Strings with hot dark matter (HDM) have been discussed by Brandenberger, Kaiser, and Turok (1987), Brandenberger, Kaiser, Schramm and Turok (1987), and Bertschinger and Watts (1988). There are some significant limitations to the work done so far –two we address in this paper are: (1) previous work has assumed a 'Newtonian Universe' –that is, the universe is dominated by non-relativistic particles and the region of space considered is much smaller than the horizon throughout the evolution period. For perturbations that are born early enough this limit will not apply. At early times relativistic particles will dominate and the horizon cannot always be assumed to be arbitrarily far away; (2) the perturbations in the string scenario come in two pieces; cosmic string and gravitational radiation from the decay of loops formed earlier. To generate a loop on of a given size there must be a corresponding absence of smaller loops formed at earlier scales. These smaller loops would have inturn become gravitational radiation. Thus where there is string there is less gravitational radiation to the extent that beyond the horizon the combined effect is zero. This leads again the problem of handling relativistic energy density. The best attempt to handle the compensating radiation has been in the most recent work of Bertschinger and coworkers who have modeled it as a uniform depression in the radiation density over the horizon at any given time (private communication). However, this does not accurately reflect the flow of the radiation and hence does not take into account the effect of the momentum flux element of the stress energy tensor. This will be explained further in section 5. The calculation in this paper avoids the earlier short comings by perturbing the relativistic generalization of the Boltzmann transport equation and Einstein's equation rather than the Newtonian approximation.

There has also been some work done on large scale structure and strings. Turok (1985) found that strings could yield a two-point correlation function for clusters that fit well with observations (Bahcall and Soneira 1983). More recent simulations indicate this effect may be smeared out through peculiar velocities of the seed loops (Bennett and Bouchet 1988). Scherrer, Melott and Bertschinger (1989) worked from a model consistent with the work of Bennett and Bouchet and were able to produce a reasonable two point correlation function when gravitational clustering was included. Concerning the large scale streaming velocities reported by Dressler *et al.* (1987), Shellard *et al.* (1987), Bertschinger

(1988), and van Dalen and Schramm (1988) all found that cosmic strings had a rather low probability of producing such a phenomenon with cold dark matter, but that hot dark matter looked more promising. The issues discussed in this paper should be especially relevant for these large scale calculations. It should be pointed out that all this work so far has ignored the effect of the infinite strings since early simulations indicated a density of about a few per horizon. More recent results (Bennett and Bouchet 1988) indicate perhaps a order of magnitude more, which would make them a major source of structure on large scales. 'Infinite' or horizon crossing strings produce wakes as they move through space. The effect of wakes has been discussed by Stebbins, Veeraraghavan, Brandenberger, Silk, and Turok (1988) and Charlton (1987).

The formalism presented in the first part of the paper will address the problem for general, spherically symmetric source perturbations. In section 2 the perturbed Boltzmann equation is derived. Section 3 will show how the equation can be interpreted as the free flow of particles plus a production term. In section 4 a model is presented for the photon/baryon fluid. It is found that the system can be treated like free flowing sound waves plus a production term analogous to that for the neutrinos. These production terms will then be defined as integrals of the perturbation in section 5.

The remainder of the paper will deal with the cosmic string scenario. Section 6 will describe the model used for the seed and underdensity. In section 7 the results are presented of a simple test for the production of galaxies and clusters. The results are then discussed and conclusions drawn in section 8.

2. The Boltzmann Equation

Lindquist (1966) shows that the relativistic generalization of the Boltzmann transport equation to be

$$\frac{dF}{dt} = p^{\alpha}\frac{DF}{dx^{\alpha}} \text{ where } \frac{D}{dx^{\alpha}} = \frac{\partial}{\partial x^{\alpha}} - \Gamma^{\beta}_{\alpha\gamma}p^{\gamma}\frac{\partial}{\partial p^{\beta}} \tag{2.1}$$

and x^{α} the space-time coordinate, t the local time coordinate, p^{α} the four-momentum, and F the phase space density.

To take advantage of the spherical symmetry, Lindquist (1966) suggests introducing an orthonormal frame or tetrad at each event. Our metric is, in time orthogonal coordinates,

$$ds^2 = -dt^2 + e^{2\Lambda}dx^2 + R^2(d\theta^2 + \sin^2\theta d\phi^2) \tag{2.2}$$

with Λ and R functions of only x and t. Λ is not to be confused with the cosmological constant, which is assumed to be zero in this work. Relative to the old basis, the new basis is

$$e_0 = e_t,\ e_1 = e^{-\Lambda}e_x,\ e_2 = R^{-1}e_\theta,\ e_3 = (R\sin\theta)^{-1}e_\phi. \tag{2.3}$$

In local spherical coordinates, taking e_1 as the polar axis, we define

$$p^0 = (p^2 + m_\nu^2)^{1/2},\ p^1 = p\cos\bar{\theta},\ p^2 = \sin\bar{\theta}\cos\bar{\phi},\ p^3 = p\sin\bar{\theta}\sin\bar{\phi}. \tag{2.4}$$

Spherical symmetry implies that $F = F(r,t,p,\mu)$ with $\mu = \cos\bar{\theta}$. $\bar{\theta}$ is the angle between the three-momentum vector and a radial vector. Reworking the algebra of Lindquist, the Boltzmann equation in full is

$$\begin{aligned}\frac{dF}{dt} = E\dot{F} + \mu p e^{-\Lambda}F' + \frac{\partial F}{\partial \mu}[\frac{R'}{R}e^{-\Lambda}p + (\frac{\dot{R}}{R} - \dot{\Lambda})E\mu](1-\mu^2)\\ - \frac{\partial F}{\partial p}Ep[\dot{\Lambda}\mu^2 + \frac{\dot{R}}{R}(1-\mu^2)] = 0\end{aligned} \tag{2.5}$$

where primes denote $\frac{\partial}{\partial x}$ and dots $\frac{\partial}{\partial t}$. We have $\frac{dF}{dt} = 0$ since the particles are collisionless.

Now, consider the metric as perturbed, flat Robertson Walker, i.e., let $e^{\Lambda} = a(1 - \frac{1}{2}h_1)$ and $R = ax(1 - \frac{1}{2}h_2)$ where a is the scale factor set to one now. With little effort one finds for the perturbed part of $F = F_0 + f$:

$$E\dot{f} + p\mu/af' - \frac{\partial f}{\partial p}Ep\frac{\dot{a}}{a} + \frac{(1-\mu^2)}{ax}p\frac{\partial f}{\partial \mu} = -\frac{1}{2}\frac{\partial F_0}{\partial p}Ep[\dot{h}_1\mu^2 + (1-\mu^2)\dot{h}_2]. \tag{2.6}$$

One can do somewhat better by letting $q = ap$. Being careful to include the change in the time derivative, one finds the momentum derivative now cancels out, leaving

$$\dot{f} + \frac{q\mu}{Ea^2} f' + \frac{1-\mu^2}{Ea^2 x} q \frac{\partial f}{\partial \mu} = -\frac{1}{2}\frac{\partial F_o}{\partial q} q[\dot{h}_1 \mu^2 + (1-\mu^2)\dot{h}_2] \tag{2.7}$$

Because the neutrinos decouple while relativistic, the background phase space density is given by

$$F_0 = \frac{2}{e^{q/q_T} + 1} \quad \text{with} \quad q_T = 1.66 \times 10^{-4} \quad eV \tag{2.8}$$

as discussed by Bond and Szalay (1984).

3. Collisionless Particles in a Flat Background

Consider a distribution of collisionless particles $g(x, q, \mu, t)$ with x, q, μ, t as defined above. Between t and $t + dt$ an element at x, q, μ moves to $x + dx, q_2 = q, \mu_2 = \mu + d\mu$.

Now, from the sine law of triangles:

$$\frac{x + dx}{\sin\theta} = \frac{x}{\sin\theta_2}$$

$$\text{hence,} \quad 1 - \mu^2 = (\frac{x+dx}{x})^2 (1 - (\mu + d\mu)^2)$$

$$\text{and} \quad d\mu = \frac{1-\mu^2}{\mu}\frac{dx}{x} = \frac{1-\mu^2}{a^2 x}\frac{q}{E} dt \tag{3.1}$$

where in the last equality we use $dx = \frac{\mu v}{a} dt = \frac{\mu q}{a^2 E}$.

The total derivative of g is thus given by

$$\frac{dg}{dt} = \frac{\partial g}{\partial t} + \frac{\partial g}{\partial x}\dot{x} + \frac{\partial g}{\partial \mu}\dot{\mu} = \dot{g} + \frac{\mu q}{a^2 E} g' + \frac{1-\mu^2}{a^2 x}\frac{q}{E}\frac{\partial g}{\partial \mu}. \tag{3.2}$$

This is the same as the left hand side of (2.7) with g replaced with f. This implies that the first order perturbation behaves like freely streaming particles that are 'squeezed' out of the comoving external medium at a rate given by the right hand side of (2.7).

With this result we have a way out of what at first sight is a very complicated partial differential equation: First, we divide space into a number of concentric shells. Then for each shell we define a grid to cover q and μ. As we time step through the evolution of this system we begin by calculating the change in the metric perturbations h_1 and h_2 (how this is done will be derived in the next section). From this we find how much perturbation is 'produced' for each x, μ, q. Finally the old and new perturbation is projected through our grid by an amount given by the momentum and the size of the time step. This is a very simple process since 'q' is an invariant for each particle and all trajectiories are straight lines.

The discussion of the last two sections follows through the same way for massless neutrinos and gravitational radiation. In these cases things are simplified by the fact that the perturbation flows at a fixed velocity. This makes it possible to reduce the number of variables by one by integrating over momentum.

Before moving on to the calculation of the metric perturbations it is worth discussing how the approach taken here relates to the Newtonian limit. In going to the Newtonian approximation one makes the redefinitions $\bar{x} = x - d$ and $\bar{t} = t - \psi$. Demanding the metric have the form

$$d^2s = -(1 - \dot{\psi})d^2\bar{t} + a^2(\bar{t})d^2\bar{x} + a^2(\bar{t})\bar{x}^2 d^2\Omega \tag{3.3}$$

and assuming $ct \gg ax$ we find $\dot{d} = \psi'/a^2$, $d = -\frac{1}{2}xh_2$, $d' = -\frac{1}{2}h_1$ and the perturbation potential $\phi = \dot{\psi}$. From here one can go either of two ways. Substituting directly into (2.7) gives

$$\frac{df}{dt} = \frac{\partial F_0}{\partial q}\frac{q}{a^2}[\psi''\mu^2 + \psi'/x(1 - \mu^2)] \tag{3.4}$$

for our Newtonian limit.

One could also work from equation (3.3) and (2.1) to get

$$\frac{df}{dt} = \frac{\partial F_0}{\partial q} m_\nu \mu \phi'. \tag{3.5}$$

This is the result of Bertschinger and Watts (1988) and Brandenberger, Kaiser, and Turok (1987). Writen out in full the left hand side looks different from the previous work because they used a different coordinate system. Here x, q, and μ were used, where $\vec{x}$ and $\vec{q}$ were used previously. The right hand side is different from (3.3) because this latter result is using comoving *background* coordinates, while in this paper we use comoving coordinates of the entire fluid. To first order in the perturbation this is not an important distinction.

4. The Photon/Baryon Fluid

After decoupling $(1+z>1300)$ the baryons are treated like cold dark matter (i.e., like neutrinos with zero velocity, since at decoupling their velocity is about 100 km/s, corresponding to a distance of approximately 0.002 Mpc in a Hubble time) and the photons are combined with the massless neutrinos. Before decoupling photons and baryons are treated as a tightly coupled fluid. A simple technique is used to model this system, which we now motivate.

To begin with, equations (85.8) and (85.9) from Peebles(1980) are combined to give

$$\frac{f}{\alpha}\frac{\partial}{\partial t}\left(\frac{\alpha}{f}\frac{\partial}{\partial t}(f\delta)-\frac{\alpha}{2}(1+\nu)\dot{h}\right)=\frac{c_s^2}{a^2}\nabla^2(f\delta) \tag{4.1}$$

where δ is the fractional perturbation in the fluid, $h=h_1+2h_2$, $c_s^2=dp/d\rho$, ρ and p are the density and pressure of the fluid, $\nu=p/\rho$, $\frac{\dot{\alpha}}{\alpha}=\frac{\dot{a}}{a}(2-3\nu)$, and $\frac{\dot{f}}{f}=-3\frac{\dot{a}}{a}(\nu-c_s^2)$. This last factor can be shown to just be due to the redshifting of the photon energy density, while the $\dot{h}$ term is the production one would expect for massless radiation plus non-relativistic matter. Defining $d\tau=\frac{f}{\alpha}dt$ we have

$$\frac{\partial^2(f\delta)}{\partial^2\tau}-\frac{\partial}{\partial\tau}\left[\frac{f}{2}(1+\nu)\frac{\partial h}{\partial\tau}\right]=\left(\frac{\alpha}{f}\frac{c_s}{a}\right)^2\nabla^2(f\delta), \tag{4.2}$$

which is very close to being just a wave equation with a source term. The equation is modeled as follows: During each time step a bit of perturbation is generated, via the $\dot{h}$ term, which then flows outward from each point of origin in spherical shells with velocity $\frac{dx}{dt}=c_s/a$. This computationally convenient interpretation is exact for a fluid of pure radiation, but with the addition of baryons the coefficient on the right side of (4.2) becomes time dependant, resulting in a dispersive system. Fortunately there are two effects that make the dispersion quite small for the system we evolve. The first is that at early times the photons dominate the fluid. The second is that at later times the region we evolve is so small relative to the horizon that the scale factor, and hence the sound speed, changes very little during the passage of a wave across the system. The dividing line between the two effects will be roughly when the comoving horizon equals the neutrino free-streaming scale, about $8h^{-2}$ Mpc. Before this time ($a_{div}\approx 1.6\times 10^{-5}$) the relevant distance scale is the horizon itself. In the time it takes to cross a horizon the scale factor doubles and one finds

$$\frac{\delta c_s^2}{c_s^2} \approx \frac{3}{4}\frac{\rho_b}{\rho_\gamma} = 0.05(\frac{a}{a_{div}})(\frac{\Omega_b}{0.1}) \qquad a < a_{div}. \tag{4.3}$$

After a_{div} the change in the scale factor in crossing the free-streaming scale is just a_{div} (in a radiation dominated universe). Hence one finds $\frac{\delta c_s^2}{c_s^2} \approx 0.05(\frac{\Omega_b}{0.1})$. Thus for small Ω_b the change in velocity is quite small.

5. Defining Equations for Metric Perturbations

Given the 'production' terms it has been shown how one can understand the fluid behavior in a simple way. Now we consider how one defines the production terms given a fluid distribution. This is done by perturbing Einstein's equations. From Peebles (1980) the relevant nonzero elements are:

$$\begin{aligned} 8\pi G T_0^0 &= 8\pi G(J_\nu + J_r + J_b + J_L) \\ &= (\frac{\dot{R}}{R})^2 + \dot{\Lambda}\frac{\dot{R}}{R} + \frac{1}{R^2} - e^{-2\Lambda}(2\frac{R''}{R} + (\frac{R'}{R})^2 - 2\Lambda'\frac{R'}{R}) \end{aligned} \tag{5.1a}$$

$$8\pi G T_1^1 = -8\pi G(K_\nu + K_r) = 2\frac{\ddot{R}}{R} + (\frac{\dot{R}}{R})^2 + \frac{1}{R^2} - e^{-2\Lambda}(\frac{R'}{R})^2 \tag{5.1b}$$

$$e^{-\Lambda}8\pi G T_0^1 = -e^{-\Lambda}8\pi G(H_\nu + H_r) = 2e^{-\Lambda}(\frac{\dot{R}'}{R} - \dot{\Lambda}\frac{R'}{R}) \tag{5.1c}$$

$$\begin{aligned} 8\pi G T_2^2 &= -8\pi G\frac{1}{2}(N_\nu + N_r - K_\nu - K_r) \\ &= \ddot{\Lambda} + \dot{\Lambda}^2 + \frac{\ddot{R}}{R} + \dot{\Lambda}\frac{\dot{R}}{R} - e^{-2\Lambda}(\frac{R''}{R} - \Lambda'^2) \end{aligned} \tag{5.1d}$$

The 'ν' subscript signifies the massive neutrino component, 'r' massless radiation, 'L' the loop, and 'b' baryons. K, H, N, and J are integrals over momentum that will be explained shortly.

To relate the equations defined in Peebles (1980) with those of Lindquist (1966) there is one subtlety that arises due to the orthonormal coordinate system. Associated with each sub/superscript of a tensor is a basis vector. When one changes the basis vectors one must make a corresponding change to the tensor. For three of the nonzero components there is no effect since the sub/superscripts are the same and the factors cancel. For T_0^1 the factor is $e^{-\Lambda}$, as indicated.

From Peebles (1980) the phase space integrals are:

$$J_\nu = 2\pi \int_0^\infty Ep^2 dp \int_{-1}^{1} d\mu F(x,a,p,\mu) \tag{5.2a}$$

$$H_\nu = 2\pi \int_0^\infty p^3 dp \int_{-1}^{1} \mu d\mu F(x,a,p,\mu) \tag{5.2b}$$

$$K_\nu = 2\pi \int_0^\infty p^4/E dp \int_{-1}^{1} \mu^2 d\mu F(x,a,p,\mu) \tag{5.2c}$$

$$N_\nu = 2\pi \int_0^\infty p^4/E dp \int_{-1}^{1} d\mu F(x,a,p,\mu) \tag{5.2d}$$

For massless radiation the defintion is the same, except that since $E = p$ the dynamic behavior of the radiation is p-independent and hence we can separate out the momentum dependence and integrate over it.

We now consider the perturbation equations. We let $e^{2\Lambda} = a^2(1-h_1)$ and $R = ax(1-h_2/2)$. The only zeroth order term that will prove useful to relate time to the scale factor is

$$(\frac{\dot{a}}{a})^2 = \frac{8}{3}\pi G J_0 \tag{5.3}$$

The first order equation for $J_1 + N_1$ (the subscript 1 will refer to the combined effect of all perturbation types) is

$$8\pi G(J_1 + N_1) = a^{-2}\partial_t(a^2(\dot{h}_1 + 2\dot{h}_2))$$

$$\text{thus} \quad \dot{h}_1 + 2\dot{h}_2 = 8\pi G a^{-2} \int_{t_i}^{t} a^2 dt (J_1 + N_1). \tag{5.4}$$

For radiation $N_1 = J_1$ while for matter $N_1 = 0$. Thus radiation will initially have twice the perturbing effect of an equal amount of cold matter. In the long run this turns out to just compensate the redshift loss to radiation energy density: The positive perturbation generated by the loop will be exactly compensated by that generated by the negative radiation perturbation.

To get an equation for $\dot{h}_2$ we first review some work of Misner and Sharp(1964). Introducing the auxiliary variable

$$m(x,t) = \frac{R}{2}(1 + (\frac{\dot{R}}{R})^2 - e^{-2\Lambda}R'^2). \tag{5.5}$$

They find from the T_0^0 equation

$$m(x,t) = \int_0^x 4\pi R^2 dx (R'J + \frac{\dot{R}}{R}H) \tag{5.6}$$

(note that we do not subscript H since $H_0 = 0$) and from the T_1^1 equation

$$\frac{\ddot{R}}{R} = \frac{G(m + 4\pi R^3 K)}{R^3}. \tag{5.7}$$

Now perturbatively,

$$\begin{aligned} LHS &= \frac{\ddot{a}}{a} - \frac{1}{2}a^{-2}\partial_t(a^2\dot{h}_2) \\ RHS &= 4\pi G(\frac{1}{3}J_0 + K_0 + \frac{1}{x^3}\int_0^x \bar{x}^2 d\bar{x}(J_1 + \dot{a}\bar{x}H) + K_1); \end{aligned} \tag{5.8}$$

hence,

$$\dot{h}_2 = \frac{8\pi G}{x^3 a^2}\int_{t_i}^t a^2 dt[K_1 + \int_0^x \bar{x}^2 d\bar{x}(J_1 + \dot{a}\bar{x}H)]. \tag{5.9}$$

Lindquist (1966) does provide a local definition of m thus making it possible to get an equation for h_2 that is local. Unfortunately it is third order in time. However, we do have the comforting result that causally disconnected regions do not influence each other. From this we conclude that $\int_0^x \bar{x}^2 d\bar{x}(J_1 + \dot{a}\bar{x}H) = 0$ for x greater than the extent of the loop/underdensity system.

In (5.9) the quantity

$$\int_0^x \bar{x}^3 d\bar{x} H = \frac{\dot{a}}{a}\int_0^x\int_0^\infty\int_{-1}^1 q^3\mu\bar{x}f d\mu dq \bar{x}^2 d\bar{x} \tag{5.10}$$

must be calculated very accurately since any error at a given radius will directly affect all shells of greater radius. Consider a piece of phase space $f(q,\mu,x,a)d\mu x^2\,dx$. We have

$$f(q,\mu,x,a)d\mu x^2\,dx = f(q,\mu_2,x_2,a+da)d\mu_2 x_2^2 \tag{5.11}$$

and from section 3

$$\begin{aligned} x_2\mu_2 &= (x+\frac{\mu q dt}{a^2E})(\mu\frac{1-\mu^2}{a^2Ex}dt). \\ &\approx x\mu + \frac{qdt}{a^2E}. \end{aligned} \tag{5.12}$$

Thus for $a \to a+da,\quad q^3\mu x f d\mu dq x^2\,dx \to q^3\mu x f d\mu dq x^2\,dx + \frac{q^4}{Ea^2} f d\mu dq x^2\,dx dt$

$$\text{i.e. } \frac{\partial}{\partial t}(q^3\mu x f) = \frac{q^4}{Ea^2}f \tag{5.13}$$

One can integrate this result to obtain

$$\frac{\partial x H}{\partial t} = N_1 \tag{5.14}$$

with N_1 as defined in section 3. The rate of change of (5.10) is thus simply the volume integral of N_1. Even though the individual particles of the photon/baryon fluid do not travel in straight lines (due to scattering) momentum is conserved and thus the coresponding quantity for this fluid must evolve similarly. Hence equation (5.14) can be used for $H_{\gamma/b}$ (δT_0^1 for the photon/baryon fluid) as well.

6. The Model and Its Parameters

Consider a comoving volume of about a cubic megaparcec or more. This volume will just enclose a loop of string (at its time of birth) big enough to seed some kind of collapsed system the size of a galaxy or larger. At the phase transition that forms the string a great deal of energy is released in other forms as well; more where there is less string. The energy density generated in its various forms will quickly smooth out on scales well inside our comoving volume. If the strings did not decay that would be the end of the story; the string becoming just another component to the background. However, due to their decay, any string that survives to a given time form isolated density contrasts. As we evolve through time our comoving volume begins to look ever lumpier, particularly after it is surpassed by the horizon. Eventually the region contains only background material or background material plus a string loop. The difference in the two possibilities is the integrated decay rate into gravitational radiation of the initial network of string. Thus a region that contains a loop produced correspondingly less gravitational radiation than a region without a loop.

The well defined parts of this story are the beginning and end. We start with no perturbation on our chosen scale, and some time later we have a loop and a corresponding deficit in gravitational radiation. For the part in-between we interpolate with the following model: The process begins at $a_s = a_{start}$ and ends at $a_b = a_{birth}$, and in-between we have the mass of the proto-loop (m_l) accumulating linearly in a. The conversion of string to gravitational radiation is a slow process, thus, so is the formation of the underdensity and string loop. How long it takes is not very important in this model. If one takes $a_s = 0.01a_b$ or $a_s = 0.001a_b$ makes little differences since in the intervening time the perturbation is of very low density relative to the background. In these calculations we used $a_s = 0.01a_b$. The total energy in underdensity is given by $\dot{E} = -\dot{m}_l - \frac{\dot{a}}{a}E$, where the last term is due to the redshifting of the radiation. The loop and negative energy radiation are created uniformly and isotropically over a sphere of fixed radius R_l. Once created the loop begins to decay into radiation at a rate given by $\gamma G\mu^2/c$ with γ =50 to 100 (Vachaspati and Vilenkin 1985).

The final relevant piece of information is the make-up of the background. We consider a universe with h =0.5, 0.75, and 1.0, h being the Hubble constant over 100 km/s/Mpc. The energy density is composed of 2.7K photons, two species of 1.9K massless neutrinos, and $\Omega_b = 0.1$ in baryons. The difference necessary to make $\Omega = 1$ is made up by one species of massive neutrino with mass given by $m_\nu = 96.8\Omega_\nu h^2 eV$.

7. Results

Since the details of the evolution of a network of cosmic strings appears to be important but not too well understood, we will forgo the usual discussion of the naive string evolution model. Instead we concentrate on the more well defined and basic problem that faces any theory for structure formation in a HDM dominated universe: Can collapsed systems be formed at scales as early as they are observed, about $a = 0.25$? The formation of Abell clusters is also examined.

a) *Galaxies and Early Forming Structure*

String simulations indicate loops tend to be born a fraction of the horizon in size and with a frequency on the order of one per horizon volume per horizon time. As a test for galaxy formation we consider a $R_l = 4$ pc loop created at $a_i = 10^{-5}$. At this scale the comoving horizon is about 4.7 Mpc, which is roughly independant of h. Concerning the size of galaxy this should seed we consider three possibilities: More than one seed of at least this size will be in this volume on average (large loop production rate), about one in this volume on average, and less than one in this volume on average (small loop production rate). The specific densities we consider are 0.00884, 0.00191, and 0.000238 loops/Mpc^3 respectively. This corresponds to one loop in a sphere of radius 3, 5 and 10 Mpc respectively. The consequence of a larger loop production rate is that there will be more loops of a given size in a unit volume and hence these loops must correspond to more numerically dense, *smaller* galaxies.

Our goal is to determine the collapse time as a function of comoving radius for shells surrounding the seed loop and to then check if a galaxy typical of the above size regions can be produced by scales as early as $a = 0.25$. We are thus interested in the size of the comoving sphere that must collapse to turn into these typical galaxies, x_{col}. We start by integrating the Schechter (1976) luminosity function with $M_B^* = -19.1 + 5\log h$, $\phi^* = 0.012h^3 Mpc^{-3}$ and $\alpha = 1.4$ (Davis and Huchra 1982) and solving for the luminosity that corresponds to the above densities. Assuming $(\frac{M}{L}) = 100$ the resulting masses are listed in Table 1. Also listed are the corresponding values of x_{col}.

The string parameters used were $G\mu/c^2 = 10^{-6}$, typical for a GUT scale, and $\beta = 9$. μ is the mass per unit length of the string and βR_l is the mean loop perimeter (Albrecht and Turok 1985).

Figures 1, 2, and 3 show the results of the simulation for $h = 1.0$, 0.75, and 0.5 respectively. The plots are of the perturbation mass interior to the comoving scale x in units of the initial loop mass. In each case a 20 Mpc sphere was considered, 200 shells and 32 directions were used, and momentum was divided into a 15 point Laguerre integral. The systems were evolved until the mean distance traveled by the massive neutrinos between then and the present was less than a shell thickness.

To estimate the time that a galaxy results we calculate the turnaround scale using the spherical collapse model. Numerical simulations indicate that a system will virialize at $t_{vir} = 1.8t_{col}$ (Peebles 1970). One finds $a_{col} = (\frac{3\pi}{4})^{\frac{2}{3}} a_i[\delta M_i(x)/M_b^i + \frac{a_i}{\dot{a}_i}\dot{h}_2^i]^{-1}$. $\delta M(x)$ is the perturbation mass interior to x, and M_b is the background mass. 'i' refers to the value at the end of the simulation. The $\dot{h}_2$ term is an addition to the usually quoted definition. It is required here since our perturbation does not start out comoving with the unperturbed background. From this the estimated collapse scales are plotted in figure 4. The scales that we want to collapse for the three values of h are indicated on each line. One need not panic at the sight of scale factors greater than one (the present) since we have some leeway in our choice of initial data. Given a factor of about five uncertainty in the mass of the seed loops, with $h = 1.0$ it is possible to seed even the largest galaxies. With $h = 0.75$ there is a cutoff at galaxies larger than $3 \times 10^{11} M_\odot$. For $h = 0.5$ only galaxies smaller than a few billion solar masses can be seeded. The large free-streaming scale, throughout the history of the loop in the $h = 0.5$ case, tends to kill the formation of larger structures.

b) *Clusters: Late Forming Structure*

Turok and Brandenberger (1985) show that the mean overdensity within an Abell radius of $1.5h^{-1}$ Mpc is about 170 times the background. This corresponds to a mean comoving sphere of background material of $8.3h^{-1}$ Mpc. Abell clusters seem to have formed relatively recently, at a scale factor of about 2/3. For our 'typical string cases' we form a loop one tenth the horizon in size when the comoving horizon equaled the mean separation of Abell clusters, $55h^{-1}$ Mpc (Bahcall and Soneira 1983). For h =1.0, 0.75, and 0.5 this corresponded to a 1000, 1700, and 3300 pc loop ,with an initial scale factor of 1.9×10^{-4}, 2.3×10^{-4}, and 3.0×10^{-4} respectively. The same values of μ and β were used.

The results for these cases are shown in figures 4, 5, and 6, again for h =1.0, 0.75, and 0.5 respectively. Using the spherical collapse model as before yields the collapse scales ploted in figure 8. As can be seen, the turnaround scale varies very little with h. This is because the mass of the region corresponding to an Abell cluster and the the size of the horizon (and hence the size of the seed loop) scale in the same way in h. Thus, given seeds about three times more massive, objects the size of Abell clusters are generic feature in this model.

8. Discussion and Conclusion

It has been demonstrated that by making a simple physical interpretation of a perturbation in a Robertson-Walker space-time how one can evolve the perturbation to first order in a relativisticly consistant manner. With this formalism it has been shown how one can study the formation of structure through cosmic string seeds without many of the approximations used in past solutions. By performing the calculation with and without these approximations the following was found: The assumption of non-relativistic neutrinos turned out to be a quite good one. Even for the $h = 0.5$ case the error is no more that 5%. A much bigger error is found when ignoring the effect of the photons and baryons before decoupling and to a lesser extent the massless neutrinos. The effect is less than 20% on galactic scales, but a factor of 2 to 3 at intermediate distances. At larger scales, ignoring massless radiation effectively negates the effect of the underdensity, since the underdensity is only relevant at early times (before it has red-shifted significantly), which is when the Universe is dominated by radiation. Consequently, if one does not properly treat the massless radiation one gets spurious perturbations developing outside the horizon. The massless radiation, whether that of the background or that of the underdensity, will have a significant effect on the large scale velocity field and should be included more carefully in future calculations.

An interesting side issue in the evolution of string seed perturbations is the mechanics of how the growth of acausal perturbations is avoided. Naively one sees a paradox since the energy in radiation drops as one over the scale factor relative to the fixed seed. Part of the resolution can be seen in equation 5.4. For matter $N_1 = 0$ while for radiation $N_1 = J_1$. One can show that, in a matter dominated Universe, after many scale factors this extra term just cancels the red-shifting loss and the total energy density perturbation sums to zero. When radiation is still important then the total energy density perturbation in fact does *not* sum to zero. This does not turn out to be a problem since the total energy density perturbation alone is never a physically meaningful quantity (unless certain other terms are zero). In equation 5.9 the energy density is joined to the term $\dot{a}xH$. Together they form a physically meaningful, conservered quantity. Since it is zero before the seed is born it remains zero and there is no acausal growth in h_2. Since 5.4 is a local equation there is also no acausal growth in $h_1 + 2h_2$ and hence the paradox is solved.

In this work a relatively naive model for the relation between cosmic string and structure was used: Each loop produces a single spherically symmetric collapsed system. However, the results of recent improved simmulations (Bennett and Bouchet 1988, Albrecht and Turok 1989) indicate a potentially much more complicated picture. The two most important new features are the large initial peculiar velocities of the loops and the larger density of string relative to previous results (Albrecht and Turok 1985). Extensions of the work presented here to more realistic situations is relatively simple. By dividing a seed perturbation into small pieces in space and time one can define the final perturbation as the sum of spherically symmetric parts, making it possible to consider arbitrary geometries. For example, one can solve the moving loop problem by considering it as a series of perturbations that exist briefly at points along its trajectory. Wakes produced behind long strings can be modeled as being seeded by a line of moving points, and a wall-like perturbation can be solved simply by integrating over each point of its surface.

I wish to thank A. Albrecht, R. P. Brinkmann, E. Bertschinger, C. Cutler, R. Rosner, D. N. Schramm, and R. Wald for helpful discussions. I further wish to especially thank Lawrence Kawano and Laurens Gunnarsen for their help and support during the occasionally difficult times over the course of this project. This work was supported by the NSF (grant No. AST85-15447) at the University of Chicago and the DOE and the NASA at Fermilab (grant No. NAGW-1340). This paper was presented to the Department of Physics, The University of Chicago, in partial fulfillment of the requirements for the Ph.D. degree.

Table 1

Comoving Volume with Mass Equal to the Largest Galaxy in a Region of a Given Size

	h =0.5		h =0.75		h =1.0	
Region (Mpc)	$\log(\frac{M}{M_\odot})$	x_{col}	$\log(\frac{M}{M_\odot})$	x_{col}	$\log(\frac{M}{M_\odot})$	x_{col}
3.0	9.15	0.165	10.57	0.375	11.18	0.494
5.0	10.37	0.421	11.13	0.567	11.59	0.677
10.0	10.99	0.678	11.56	0.801	11.92	0.872

REFERENCES

Albrecht, A. and Turok, N. 1985, Phys. Rev. Lett. **54** 1868.

Albrecht, A. and Turok, N. 1989, Fermilab preprint.

Bahcall, N.A. and Saneira, R.M. 1983, Astrophys. J. **270**, 20.

Bennett, D.P. and Bouchet, F.R., 1988, Phys. Rev. Lett. **60** 257.

Bertschinger, E. and Watts, P.N. 1988, Astrophy. J. **328**, 23.

Bond, J. and Szalay, A. 1984, Astrophys. J. **274**, 443.

Bouchet, F., Bennett, D. and Stebbins, A. 1988, Fermilab preprint.

Brandenberger, R.H., Kaiser, N., Schramm D.N. and Turok, N. 1987, Phys. Rev. Lett. **59**, 2371.

Brandenberger, R.H., Kaiser, N. and Turok N. 1987, Phys. Rev. D **36**, 2242

Charlton, J.C. 1988, Astrophys. J. **325**, 521.

Davis, M. and Huchra, J.P. 1982, Astrophys. J. **254**, 437.

de Lapparent, V., Geller M.J., and Huchra, J.P. 1986, Astrophys. J. (*Letters*), **302**, L1.

Dressler, A., Faber, S.M., Burstein, D., Davis, R.L., Lynden-Bell, D., Terlevich, R. and Wegner, G. 1987, Astrophys. J. (Letters) **313** L37.

Frenk, C.S., White, S.D.M. and Davis, M. 1983, Astrophys. J. **271**, 417.

Kibble, T.W.B. 1976, J. Phys. **A9**, 1387; Phys. Rep. **67**, 183 (1980).

Lindquist, R.W. 1966, Ann. of Phys. **37**, 487.

Misner, C.W. and Sharp, D.H. 1964, Phys. Rev. **136**, B571.

Peebles, P.J.E. 1970, Astrophys. J. **75**, 13.

Peebles, P.J.E. 1982, Astrophys. J. **258**, 415.

Peebles, P.J.E. 1980, The Large-Scale Structure of the Universe (Princeton University Press).

Sato, H. 1986, Prog. Theor. Phys. **75**, 1342.

Schechter, P. 1976, Astrophys. J. **203**, 297.

Scherrer, R.J., Melott, A.L. and Bertschinger, E. 1989, Phys. Rev. Lett. **62**, 379.

Shellard, E.P.S., Brandenberger, R. H., Kaiser, N. and Turok, N. 1987, Nature **326**, 672.

Schramm, D.N. 1985, p. 181, The Cosmic Background Radiation and Fundamental Physics ed. F. Melchiorri (Italian Physical Society, Bologna).

Stebbins, A. 1986, Astrophys. J. (Letters) **L21**, 303.

Stebbins, A., Veeraraghavan, S., Brandenberger, R., Silk, J. and Turok, N. 1987, Astrophys. J. **322**, 1.

Turok, N. 1985, Phys. Rev. Let. **55**, 1801.

Turok, N. and Brandenberger, R. 1986, Phys. Rev. **D33** 2175.

van Dalen, A. and Schramm, D.N. 1988, Astrophys. J. **326**, 70.

Vachaspati, T. and Vilenkin, A. 1985, Phys. Rev. D **31**, 3052.

Vilenkin, A. 1981, Phys. Rev. Lett. **46**, 1169.

Zel'dovich, Y.B. 1980, Mon. Not. R. Astr. Soc. **192**, 633.

FIGURE CAPTIONS

1. Mass function vs scale at $a = 0.1$: $h = 0.5$, 4 pc loop, $a_{born} = 1 \times 10^{-5}$

2. Mass function vs scale at $a = 0.1$: $h = 0.75$, 4 pc loop, $a_{born} = 1 \times 10^{-5}$

3. Mass function vs scale at $a = 0.02$: $h = 1.0$, 4 pc loop, $a_{born} = 1 \times 10^{-5}$

4. Turnaround Scale vs radius: 4 pc loop, $a_{born} = 1 \times 10^{-5}$

5. Mass function vs scale at $a = 0.1$: $h = 0.5$, 1000 pc loop, $a_{born} = 1.9 \times 10^{-4}$

6. Mass function vs scale at $a = 0.1$: $h = 0.75$, 1700 pc loop, $a_{born} = 2.3 \times 10^{-4}$

7. Mass function vs scale at $a = 0.02$: $h = 1.0$, 3300 pc loop, $a_{born} = 3.3 \times 10^{-4}$

8. Turn around Scale vs radius, $h = 1.0$: 1000 pc loop, $a_{born} = 1.9 \times 10^{-4}$, $h = 0.75$: 1700 pc loop, $a_{born} = 2.3 \times 10^{-4}$, $h = 0.5$: 3300 pc loop, $a_{born} = 3.0 \times 10^{-4}$

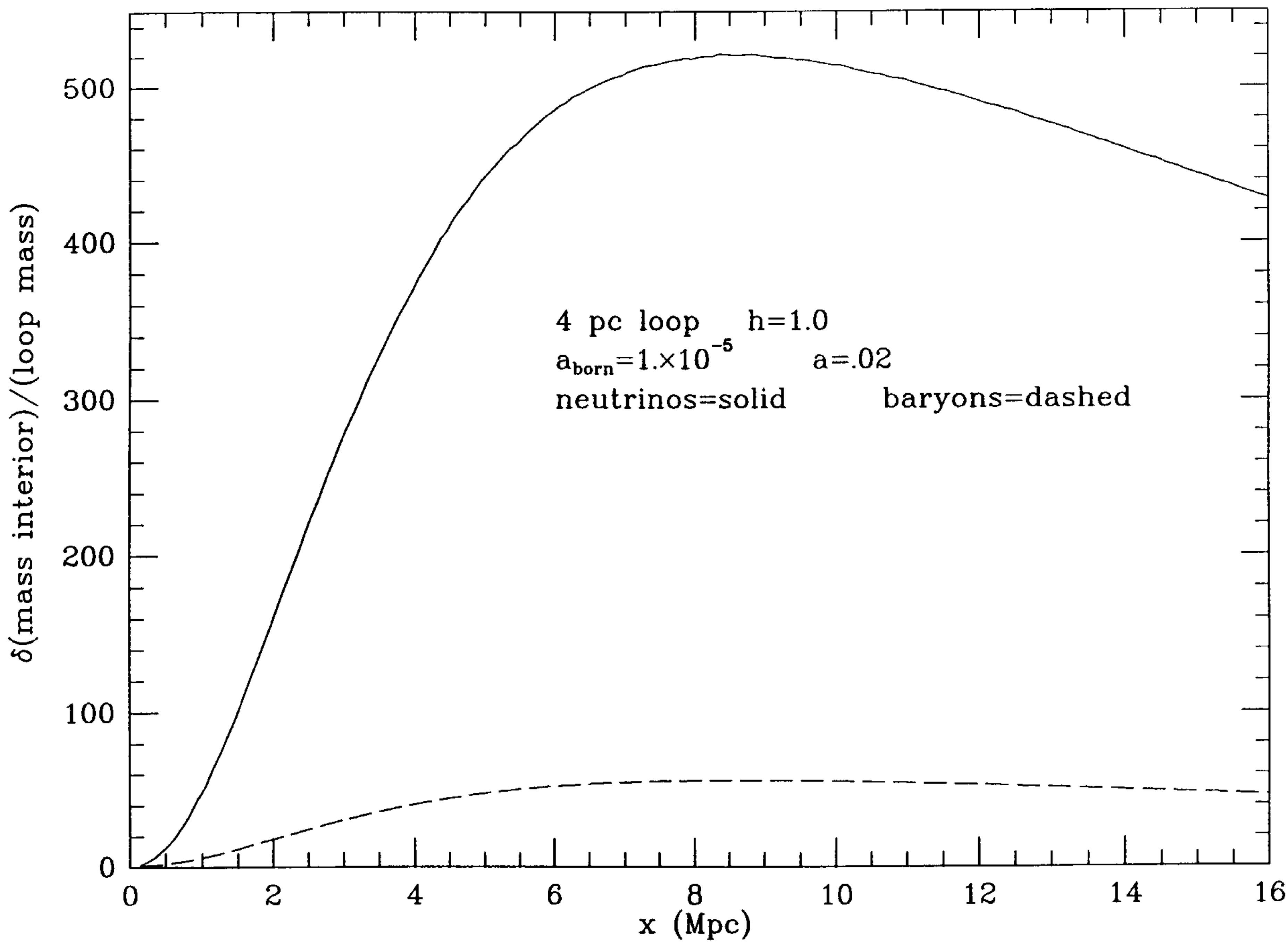
4 pc loop h=1.0
$a_{born}=1.\times10^{-5}$ a=.02
neutrinos=solid baryons=dashed
δ(mass interior)/(loop mass)
x (Mpc)
0
100
200
300
400
500
0
2
4
6
8
10
12
14
16

Figure 1.

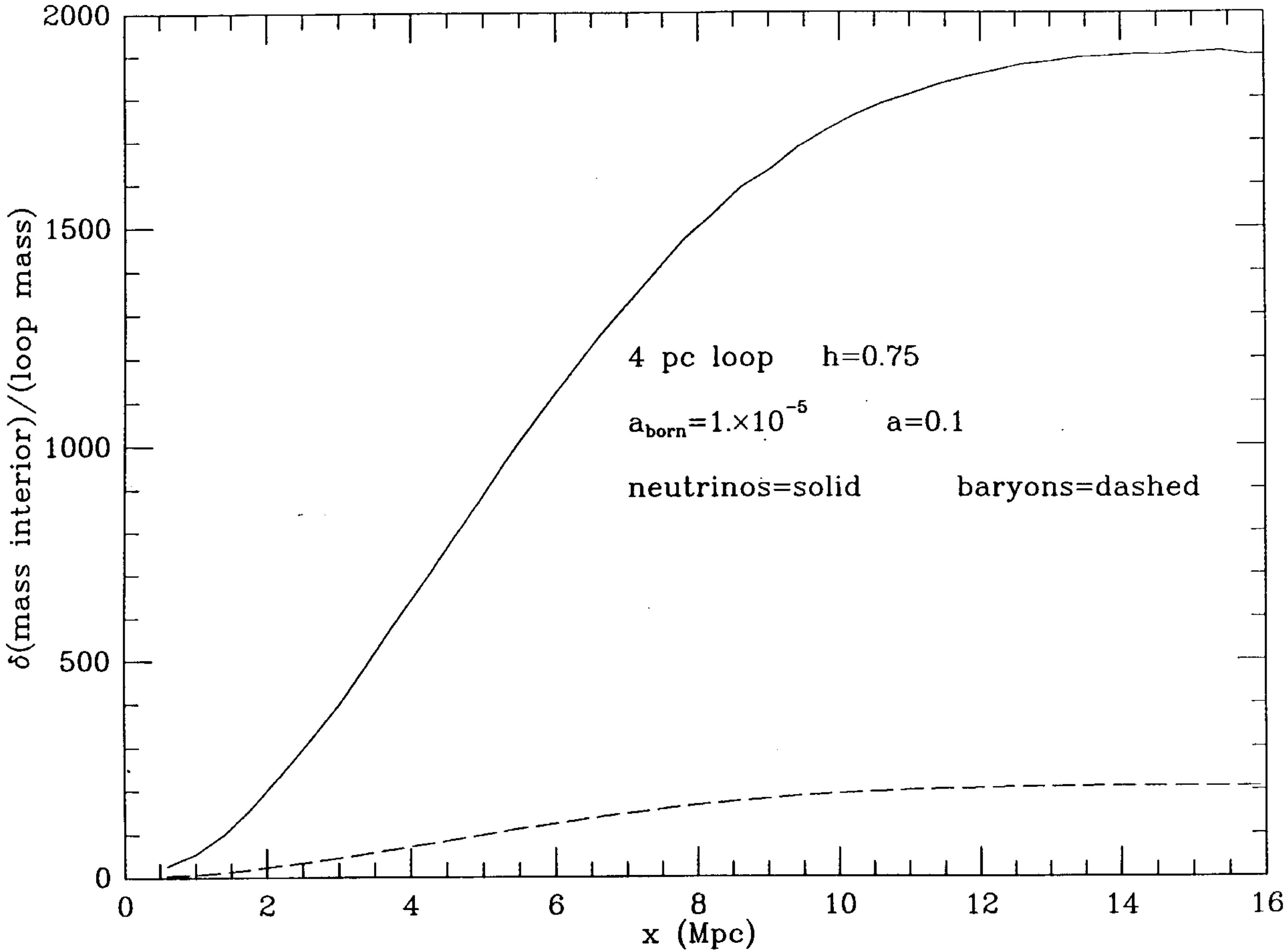

2000
1500
1000
500
0
0
2
4
6
8
10
12
14
16
x (Mpc)
δ(mass interior)/(loop mass)
4 pc loop h=0.75
$a_{born}=1.\times10^{-5}$ a=0.1
neutrinos=solid baryons=dashed

Figure 2.

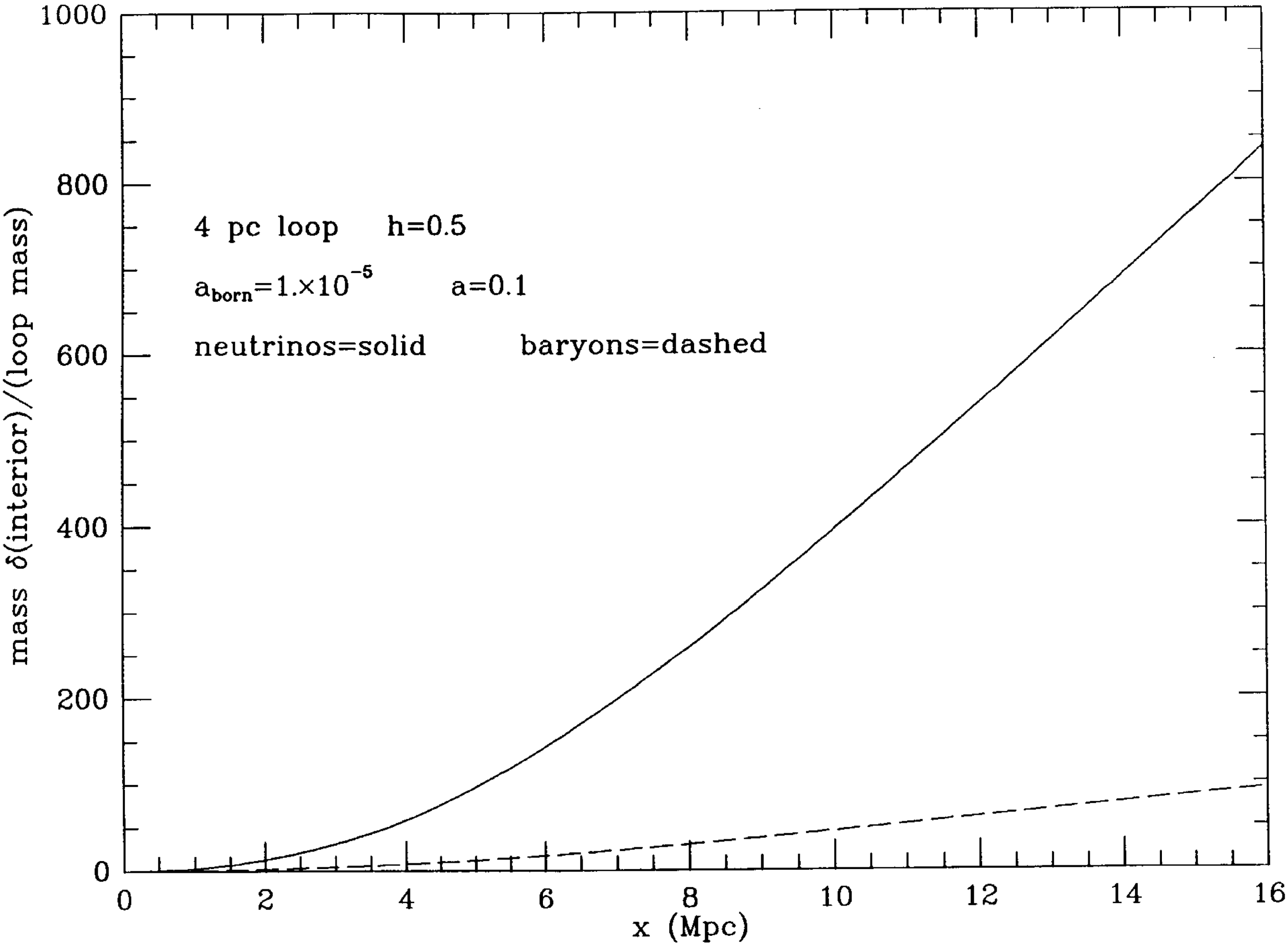

4 pc loop h=0.5
a_born=1.×10^-5 a=0.1
neutrinos=solid baryons=dashed
mass δ(interior)/(loop mass)
x (Mpc)
0
200
400
600
800
1000
0
2
4
6
8
10
12
14
16

Figure 3.

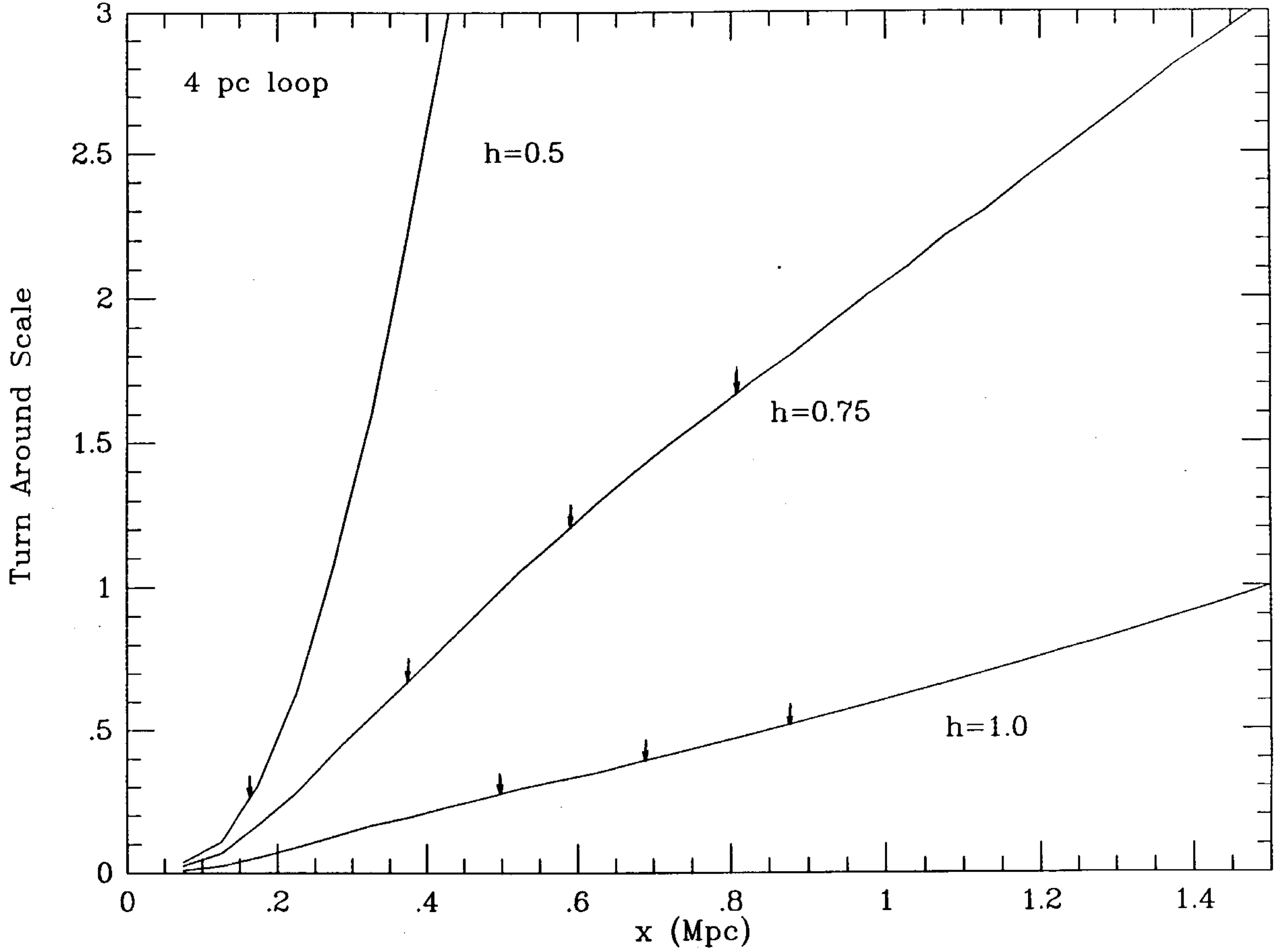
4 pc loop
h=0.5
h=0.75
h=1.0
Turn Around Scale
x (Mpc)
0
.5
1
1.5
2
2.5
3
0
.2
.4
.6
.8
1
1.2
1.4

Figure 4.

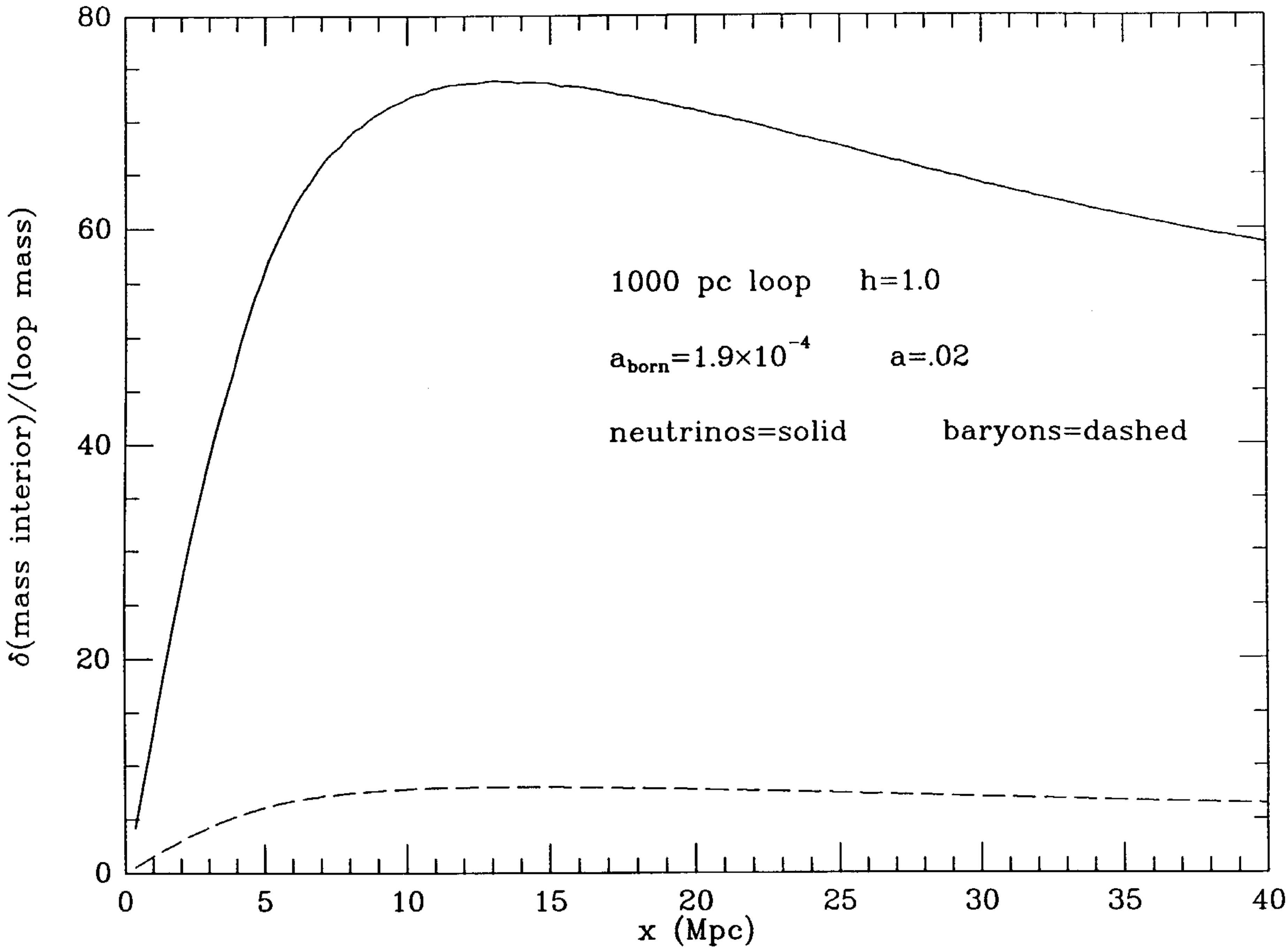
1000 pc loop h=1.0
a_{born}=1.9×10^{-4} a=.02
neutrinos=solid baryons=dashed
δ(mass interior)/(loop mass)
x (Mpc)
0
20
40
60
80
0
5
10
15
20
25
30
35
40

Figure 5.

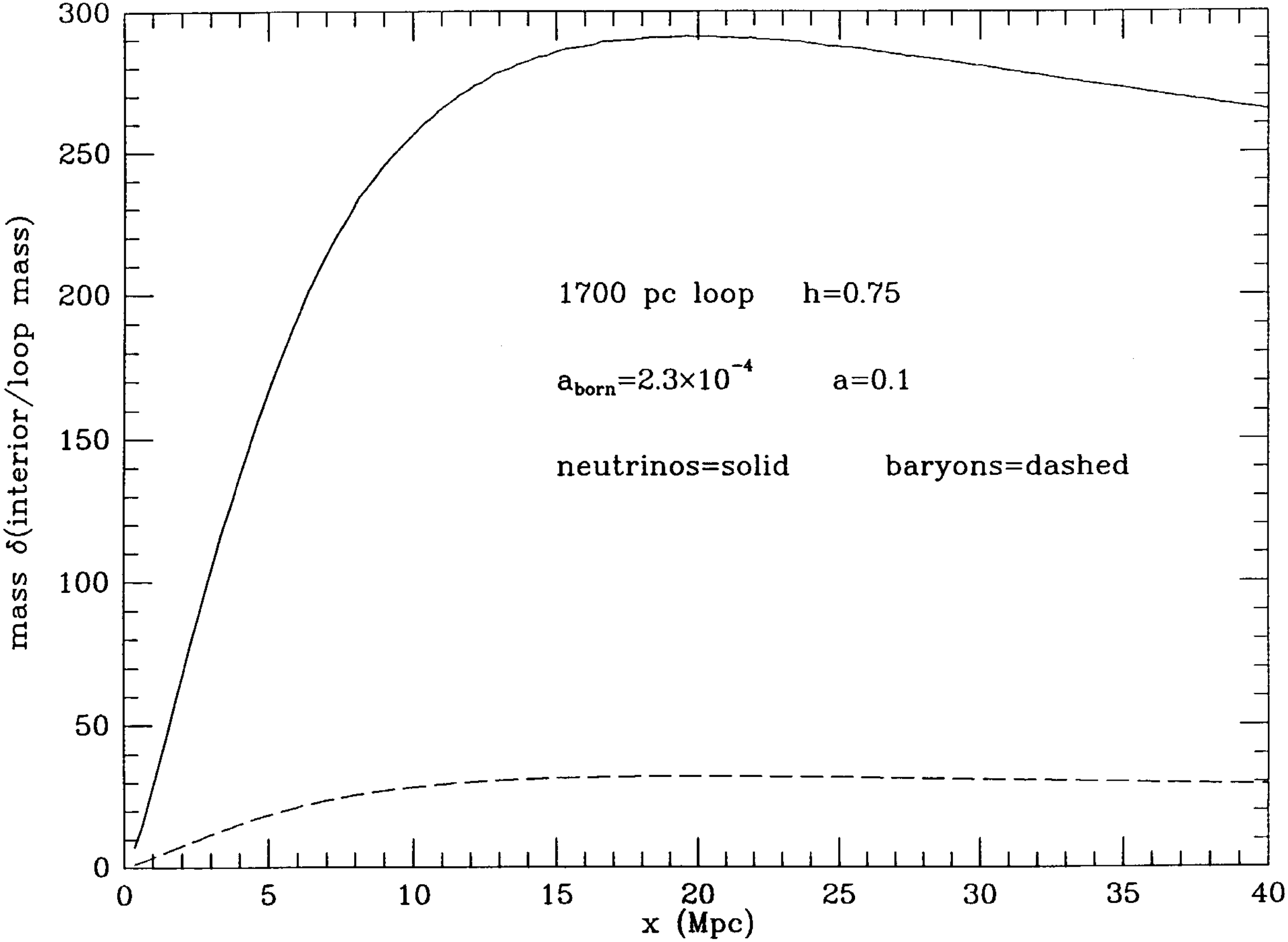
1700 pc loop h=0.75
$a_{born}=2.3\times10^{-4}$ a=0.1
neutrinos=solid baryons=dashed
mass δ(interior/loop mass)
x (Mpc)
0
50
100
150
200
250
300
0
5
10
15
20
25
30
35
40

Figure 6.

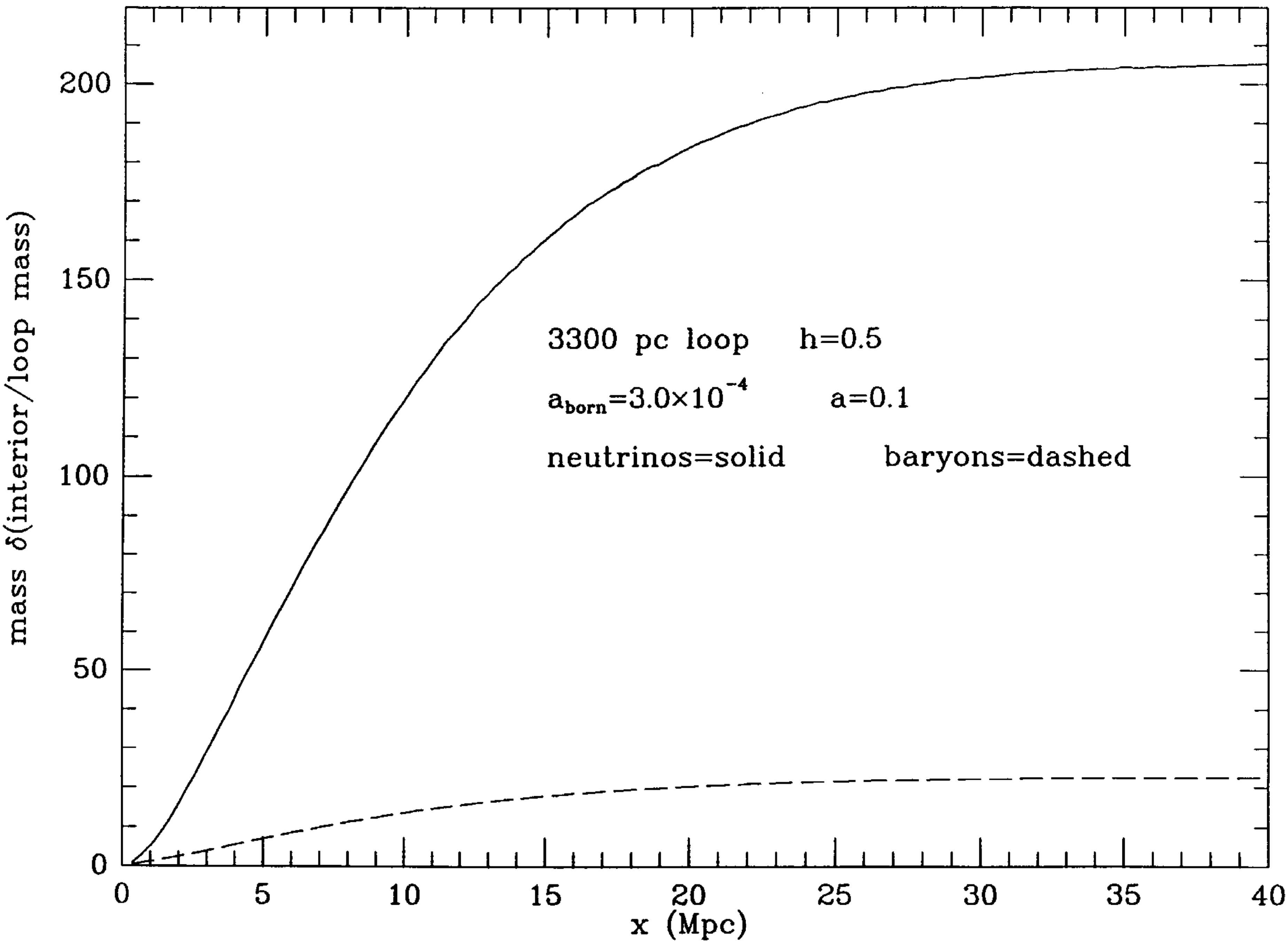
3300 pc loop h=0.5
a_born=3.0×10^-4 a=0.1
neutrinos=solid baryons=dashed
mass δ(interior/loop mass)
x (Mpc)
0
50
100
150
200
0
5
10
15
20
25
30
35
40

Figure 7

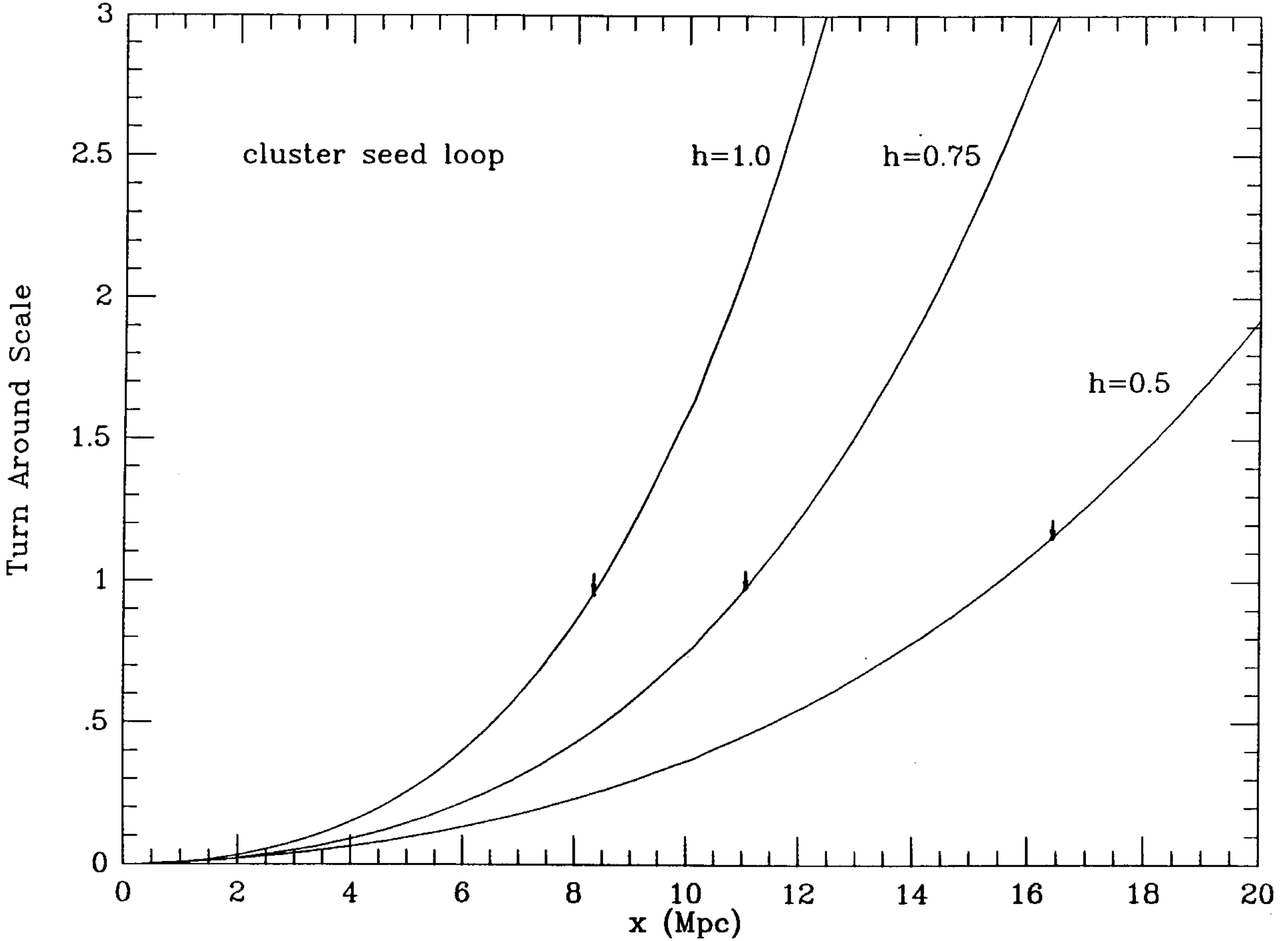
3
2.5
2
1.5
1
.5
0
Turn Around Scale
cluster seed loop
h=1.0
h=0.75
h=0.5
0
2
4
6
8
10
12
14
16
18
20
x (Mpc)

Figure 8.

POSTAL ADDRESS

Anthony van Dalen
Department of Physics
The Ohio State University
174 West 18th Avenue
Columbus OH 43210-1106